FEASIBILITY DEMONSTRATION OF A 445N HIGH-PERFORMANCE ROCKET ENGINE

Marshall A. Appel
Jet Propulsion Laboratory
California Institute of Technology
Pasadena, California

Leonard Schoenman
Dr. Jerrold E. Franklin
P. Tina Lansaw
Aerojet TechSystems Company
Sacramento, California

ABSTRACT

A program to demonstrate the feasibility of a high-performance 445 Newton (100 lb_f) NTO/MMH rocket engine was the object of a JPL contract with the Aerojet TechSystems Company. An existing high-performance injector was coupled with three different thrust chambers to acquire test data for the program. A stainless-steel sea-level chamber was used for test stand checkout, calibration and initial injector performance determinations. Two high-temperature iridium lined rhenium thrust chambers were used to determine altitude performance and durability. The first chamber was tested for a total duration of 3381 s and the second was tested for a total duration of 15,000 s with no measurable degradation. Extrapolation of ϵ = 44:1 experimental data to the recommended ϵ = 467:1 expansion nozzle, using the JANNAF methodology, showed that a performance of 3138 to 3167 N-s/kg (320 to 323 lb_f-s/lb_m) could be achieved with the present design. Recommendations are presented which would allow a redesigned engine to achieve the 3195 N-s/kg (326 lb_f-s/lb_m) program goal.

INTRODUCTION

The Mariner Mark II Spacecraft represents a new generation of low-cost, generic space probes designed for the purpose of exploring the Solar System. Numerous missions such as CRAF, CASSINI, MBAR, and UFUP are planned. All will use slight modifications of a standardized bus design. The missions for these probes defined by Draper[1,2] include:

CRAF = Comet Rendezvous Asteroid Flyby

CASSINI = Saturn Orbiter and Titan Probe

MBAR = Main Belt Asteroid Rendezvous

UFUP = Uranus Flyby and Uranus Probe

A typical spacecraft, such as that shown in Fig. 1, would have a dry weight of 1200 to 1600 kg and carry on the order of 3000 to 4000 kg of propellants to attain the required trajectories and orbit insertions.

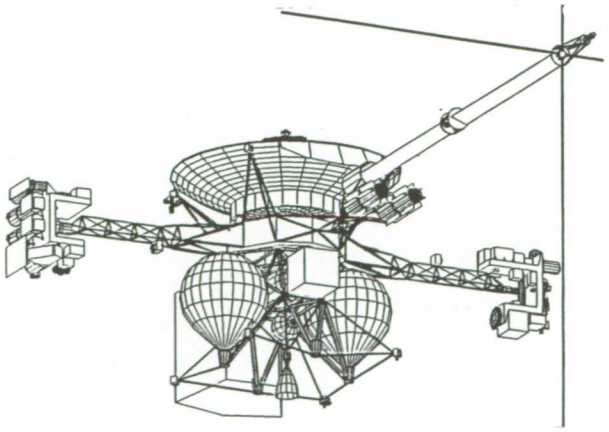

Figure 1. CRAF Spacecraft Configuration

---

* The research described in this paper was carried out by the Jet Propulsion Laboratory, California Institute of Technology, under contract with the National Aeronautics and Space Administration. Approved for public release; distribution unlimited.

Since over 75% of the weight of the fully loaded spacecraft is propellants, even small improvements in propulsion efficiency can yield a large increase in the number of experiments. For example, an analysis of the CRAF spacecraft mass, Reference 1, indicated that incorporation of a high-performance rocket engine, I_{sp} = 3195 N-s/kg (326 lb_f-sec/lb_m), into the propulsion system could have resulted in a reduction of spacecraft wet mass by approximately 600 kg. This would have enabled the addition of three experiments to the 14-experiment, 13-instrument science payload.

GOALS AND OBJECTIVES

The objective of this rocket engine feasibility demonstration program was to demonstrate a 5% improvement in propulsion efficiency over the baseline Galileo engine which can provide a specific impulse of 2994 N-s/kg (308 lb_f-sec/lb_m). The engine operating parameters and design goals are listed in Table I.

TABLE 1. DESIGN GOALS FOR HIGH-PERFORMANCE ENGINE

		Goals
Primary:	Propellants	N_2O_4/MMH
	Thrust, Vacuum	445N (100 lb_f)
	Specific Impulse	3195 N-s/kg (326lb_f-s/lb_m)
	Life	> 12 hr
	Number of Starts	> 100
	Gimballing	± 9° in two axes
Secondary:	Inlet Pressure	< 1587 kN/m^2 (230 psia)
	Mass (including valves)	< 3.2 kg (7 lb)
	Length	< 50.8 cm (20 in)

BACKGROUND AND TECHNICAL APPROACH

The significant improvement in performance over existing engine designs was to be achieved through the use of a highly efficient platelet injector, Energy Release Efficiency (ERE) >99%, combined with an advanced high-temperature chamber material system which would operate with a minimum use of fuel film cooling, and by the addition of a larger, more efficient high expansion nozzle. A major reduction in the quantity of fuel film cooling required the use of a chamber material which could operate at temperatures significantly higher than the 1316°C (2400°F) limit of silicide-coated columbium, the USA industry standard, and the 1538°C (2800°F) limit of platinum alloys, which have been successfully demonstrated at Aerojet. A radiation-cooled engine which operates without supplemental fuel film cooing would reach an equilibrium temperature of approximately 1927°C (3500°F).

The elimination of fuel film cooling also requires the development of a thermal management system which allows joining of the hot chamber to a cold injector and valve and controls the post-fire heat soak-out without compromising the low residual propellant volume between the valve seat and injector face. The low residual volume is essential for contamination-free shutdown and pulse mode capability. The solutions to these design requirements are not trivial.

Prior to this program, JPL had successfully designed, fabricated, and tested film-cooled rhenium chambers operating at approximately 1649 to 2205°C (3000 to 4000°F) with liquid fluorine/hydrazine and gaseous oxygen/hydrogen propellants[3,4,5]. Aerojet had determined under IR&D that rhenium could operate successfully at 2205°C (4000°F) at low NTO/MMH mixture ratios, but was not sufficiently oxidation resistant to operate at the 1.65 value required for optimum spacecraft performance. The material was also unsuitable for applications requiring pulse-mode operation for extended periods. Aerojet had also investigated the use of iridium-clad rhenium as a means of extending operation to pulse-mode applications and to higher combustion O/F ratios, and reached the conclusion that this material system does not require film cooling and works best when the combustion efficiency is very high, i.e., a streaking or low-performing injector is unacceptable.

Prior to the start of this program, the Ultramet Company had independently developed a CVD process which appeared capable of producing a rhenium combustion chamber containing an iridium liner. A joint Aerojet/Ultramet effort had demonstrated that their process could produce a 22 Newton (5-lb_f) class thrust chamber material that could operate for 8 hours at 2205°C (4000°F) at O/F ratios of 1.65, provided that the oxidizer was fully combusted.

The 22 Newton (5-lb_f) engine design, fabrication, and test data base was subsequently reproduced and expanded by Aerojet to demonstrate 15 hours of operation at 2205°C (4000°F)[6]. The measured specific impulse of the 22 Newton (5-lb_f) engine was 3014 N-s/kg (310 lb_f-sec/lb_m) when tested with a 150:1 expansion ratio nozzle.

A successful and timely demonstration of both performance and durability at the 445 Newton (100-lb_f) thrust level was dependent on two key factors: 1) Ultramet's ability to scale up, by a factor of 20, the iridium/rhenium high-temperature chamber and 2) on the availability of an injector that could provide near-perfect propellant mixing and combustion efficiency. The Aerojet patented platelet injector and a proprietary combustion chamber configuration (patent pending) provided the only known approach to meeting these stringent performance requirements. Aerojet had independently designed and fabricated a high element density (4.4 Newton (1 lb) thrust per element) platelet injector which was capable of providing the required thrust/pressure design goals, chamber wall compatibility, and very high performance. This injector and a close-coupled Moog series redundant torque motor bipropellant valve, Fig. 2, were supplied by Aerojet at the start of this 13-month feasibility demonstration program.

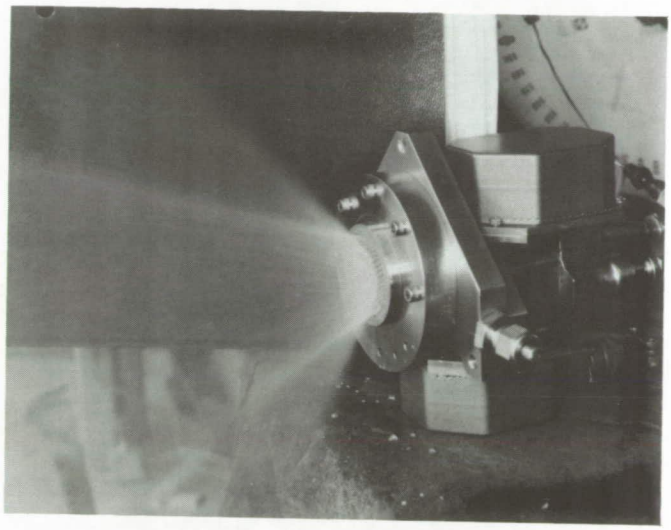

Figure 2. Series Redundant Torque Motor Bipropellant Valve and Platelet Injector During Cold-Flow Inspection of One of Two Propellant Circuits

This high-performance engine feasibility demonstration program consisted of an iterative design, fabrication, test, and data analysis process.

TEST HARDWARE DESIGN AND DESCRIPTION

Figure 3 shows the test engine assembly with the ϵ = 44:1 area ratio nozzle in a horizontal firing position in the vacuum test cell. Figure 4 shows the face of one of the three 92-element splash plate injectors after 5 hours of burn time and over 100 starts. Table II itemizes the important features of this design. Each injector contains 2 pressure ports, one of which is fitted with a close-coupled Kistler high-frequency transducer. The injector/chamber assembly provides acoustically tuned resonator cavities to attenuate organized pressure waves which could lead to combustion instabilities. Figure 4 also shows 16 replaceable set screws located within the resonator cavity around the periphery of the injector. Each set screw contains a precise laser machined orifice and an inlet screen to prevent orifice plugging. The replaceable set screws provide a simple method of systematically reducing the fuel film coolant flow and adjusting the flow distribution in order to maximize the performance using a single injector. Screw sets consisting of unorificed, 96 μm (0.0038 in.), and 125 μm (0.0049 in.) orificed assemblies provided the capability of adjusting the fuel film cooling from 0 to 11% of the fuel. The platelet injector also contains internal screens to protect the 187 orifices. These are in addition to the filters contained within the valve body at the valve inlet.

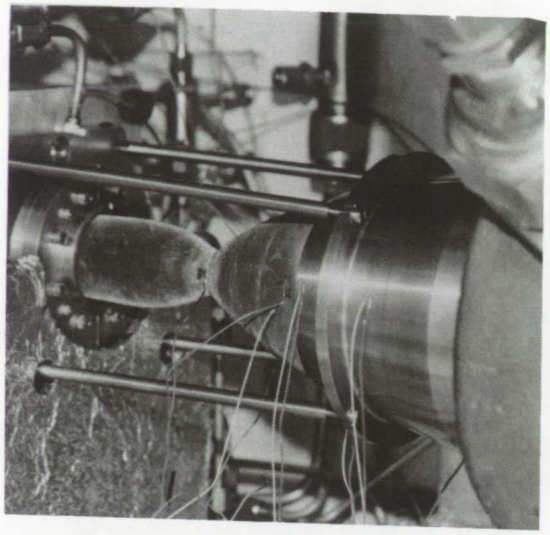

Figure 3. 445N (100 lb_f) Engine with 44:1 Nozzle Extension Mounted in Vacuum Test Cell

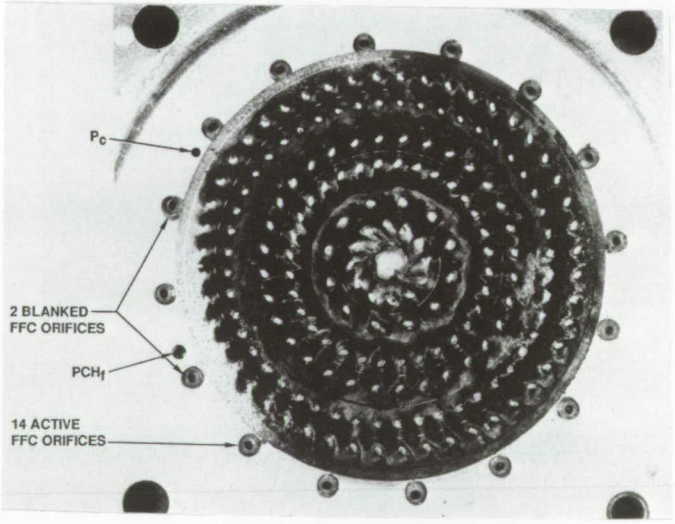

Figure 4. Injector Following 18,382 s of Burn Time and 97 Full Thermal Cycles

TABLE II. FEATURES OF HIGH-PERFORMANCE PLATELET INJECTOR

Material of Construction:	Corrosion-Resistant Stainless Steel
Element Type:	Unlike Doublet
Orifice Type:	Self-Atomizing Splash Plate
Number of Active Fuel Orifices:	95
Number of Active Oxidizer Orifices:	92
Fuel Orifice dia, cm (in.)	0.018 (0.007)
Oxidizer Orifice dia, cm (in.)	0.020 (0.008)
Injector Dia, cm (in.)	4.34 (1.71)
Film Cooling Orifices:	Variable, 0 to 16, 0 to 11% FFC

Anti-Plugging Screens in Core and Coolant Orifices
Chamber Pressure Measurement Port
Close-Coupled Kistler High-Frequency Pressure Transducer Port
Critically Damped Acoustic Resonators

In the test assembly, a fuel regeneratively cooled transition section was positioned between the injector and the combustion chamber. The transition section functions as a thermal management device and enables welding of the hot chamber to a cold injector for the flight configuration. The regenerative section also recovers some of the heat that would be lost by radiation from the hot chamber and provides a method of attaching the engine to the spacecraft without requiring the spacecraft to accept a thermal load at the interface. The final design of the fuel regenerative transition section was preceded by calibration testing with a highly instrumented water-cooled calorimetric section which completely defined the convection and conduction heat loads.

A bolted assembly was employed for the feasibility demonstration. The engine thermal model indicated that the bolted assembly tested produced a more severe thermal soak environment than an all-welded flight design because of the large conduction path surfaces required to make the seals. A Grafoil seal material was employed at the hot chamber interface to partially offset the large contact area.

Two heat sink steel chambers having identical 1.6:1, 15 degree half-angle expansion cones, but different overall lengths provided a method of checking out the injectors, providing combustion stability and sea level performance data. Some sea level test assemblies were fitted with 75-μm (0.003 in.)-thick rhenium foil chamber inserts to verify chamber wall compatibility. An Aerojet-developed exhaust plume analyzer was provided to monitor the presence of rhenium in the gas stream during startup, steady-state operation, and shutdown. Inspection of the foil condition and its pre- to post-test weight change, in conjunction with the plume data, allowed performance maximization without the risk of creating chamber wall incompatibilities which could show up later in the durability testing. Figure 5 shows a typical sea level engine assembly in operation.

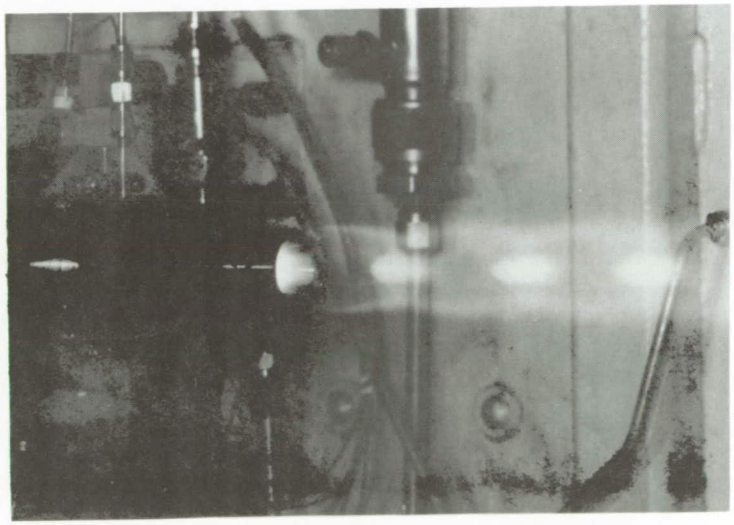

Figure 5. Sea Level Test Configuration for Stability and Performance Evaluation and Exhaust Plume Monitoring for Potential Chamber Wall Degradation

The head end of the high-temperature chamber, shown in Fig. 3, was identical to the heat sink steel chamber, but extended to an expansion ratio of 22:1. The aft end provided for the attachment of a stainless steel nozzle extension which created an optimum expansion, 44:1, 90% bell nozzle for the purpose of obtaining accurate thrust-based performance data. Figure 3 also shows the method of retaining the extension using 4 tie rods and springs. The skirt was designed to be removed for the durability testing because it allowed significantly longer test time in the vacuum test cell without encountering nozzle flow separation.

CHAMBER FABRICATION SCALE-UP

The iridium-lined rhenium chambers were fabricated by the Ultramet Company using their proprietary CVD process, but not without difficulty. The processing parameters that worked satisfactorily for the smaller 22 Newton (5-lb_f) engines could not provide a sufficiently thick iridium layer to meet the design thickness required to satisfy the 12 hour life goal. The application of multiple iridium layers resulted in cracking and interlayer disbonds that had not been experienced on smaller nozzles. After some failures, it became evident that the time and funding required to develop the optimum processing parameters were beyond the program scope and schedule limitations. Two fireable units with known imperfections, however, were delivered and accepted on a best-effort basis. The first had multiple thin layers which, in combination, added up to only 50% of the thickness of the single layer which

demonstrated a 15 hour life at 22 Newtons (5-lb_f). The second had fewer layers adding up to the desired total thickness in the chamber and throat region, but almost no protection in the last 7.62 cm. (3 in.) of the skirt because the iridium cracked and spalled during fabrication and had to be removed. In addition, x-ray and dye penetrant inspection showed coating cracks in the iridium in the forward seal area and also adjacent to the skirt region where the spalled iridium had been mechanically removed. These same inspection processes indicated that the entire combustion chamber through the throat was free of measurable defects.

TEST PROGRAM

The test program consisted of four phases: (1) cold flow checkouts, (2) short (7-s) hot-fire checkout tests at sea level with the instrumented, steel heat sink throat and rhenium foil lined chamber assembly to verify stable combustion, fuel-cooled head end operation, and chamber wall capability, (3) longer-duration (approximately 60 s) performance and thermal mapping tests in the vacuum test cell using the iridium-lined rhenium chamber and the ϵ = 44:1 clamp-on steel heat sink skirt, and (4) long-duration (500 to 800 s) vacuum cell durability testing without the steel skirt.

TEST FACILITY AND INSTRUMENTATION

Testing was conducted in the Aerojet Research and Engineering Development Laboratory. This test facility contains a 311.5 m^3 (11,000 ft^3) mechanically pumped altitude test cell (.069 KN/m^2(0.01 psi) at start), a 15.24 cm (6-in.)-dia. cooled diffuser, two .152 m^3 (40-gal) stainless steel propellant tanks, a helium pressurization system, and a propellant thermal conditioning system.

The propellant supply was sufficient for single burns of approximately 2000 s. The vacuum facility limited the maximum single-burn duration to 500 to 800 s. The MMH fuel and NTO-Mon-3 oxidizer were per MIL P27404B and MIL P26539, respectively. Five μm filtration was employed in transferring the oxidizer from the large propellant delivery trailer to the stainless steel run tanks. No special provisions were made to remove the ferric nitrate from the oxidizer. Post-test propellant analyses indicated 2.9 ppm ferric nitrate, 2.4 w% NO, and 0.14 w% H_2O in the oxidizer. The fuel was 98.8 w% MMH and 0.12 w% H_2O.

Instrumentation consisted of 4 channels for propellant flow, 24 channels for pressure and thrust, 24 channels for temperature, and an independent high-frequency FM recording system for dynamic pressure. Two Ircon 2-wavelength optical pyrometers and an infrared full-view Thermovision system provided maximum temperatures and hot-spot locations. The data acquisition system was a NEFF-620 Model 100 capable of recording 32,000 data points each second.

Critical performance measurement parameters, i.e., propellant flow, thrust, and vacuum cell pressure, were redundant. This included the temperature and pressure compensated Class 1 dual bridge load cell, two fuel and two oxidizer turbine type flow meters in series, and two low-range vacuum cell pressure transducers. The turbine type flow meters were calibrated on the test stand with propellants using a piston travel time-volume standard. The dual bridge load cell was provided from the Aerojet Measurement Standard Laboratory with NBS traceable dead weight calibrations. A reference load cell having similar calibrations was also positioned within the test cell. On-line pre- and post fire calibrations were conducted at vacuum with the propellant lines pressurized by applying a series of 4 load steps on the engine thrust frame using an automated pneumatic actuation system. This external force along the engine thrust centerline results in the dual load cells and reference cells being loaded in series and provides a mechanism to correct the measured thrust for external drag on the thrust frame. An external calibration was also performed at the start of the test series by the use of a third load cell in place of the engine.

Based on a large statistical data base for the test system, the expected three sigma measurement uncertainty is:

Force $\pm$ 0.5%

Flow $\pm$ 0.5%

Vacuum Cell Pressure $\pm$ 0.3%

Analysis of the data from the first 12 performance mapping tests indicated the one sigma combined calibration and measurement uncertainty was less than 0.2% or approximately 5.9 N-s/kg (0.6 lb_f-sec/lb_m).

EXPERIMENTAL RESULTS

A total of 147 engine firings were conducted. Of these, 74 were sea level tests of 7 s duration each, 28 were 30 to 90 s thermal and performance tests in vacuum with the 44:1, 90% bell nozzle attached, and 43 were durability tests of up to 800 s each, also in vacuum but without the nozzle extension.

Stability No evidence of combustion instability was encountered in the 147 firings. Stable combustion was provided by the use of tuned acoustic resonator cavities. Stability was monitored via a Kistler high-frequency transducer located within the resonator cavity.

Flow Decay No evidence of oxidizer flow decay was experienced in over 5 hours of accumulated burn time. Most of the testing was conducted at a ferric nitrate level of approximately 3 ppm. No platelet injector has ever experienced a flow decay problem.

Propellant Depletion and Gas Injestion Tests This type of testing was not included in the program scope. However, in one of the long-duration durability tests, the NTO tank ran dry and an undefined degree of gas ingestion was encountered. The engine was shut down when a large drop in thrust was noted. No damage was encountered to either the injector or the chamber.

Two tests in which a gas bubble of undefined origin was present in the fuel line at startup were also experienced. These tests were also terminated by the lower red-line limits on chamber pressure without damage to the engine.

During one of the many fuel tank refills, a massive amount of large particle and small particulate contaminated fuel entered the run tank. This resulted in significant obstruction of the facility filter at the valve inlet and also the filter internal to the valve. This made it impossible to maintain mixture ratio. After cleaning the valve and facility filters, but not the filters internal to the injector, the injector valve assembly was cold flowed and the pattern visually inspected. This inspection indicated the injector pressure drop and flow distribution, including the fuel film coolant were unaffected by the contamination and the engine internal protective system was operating effectively.

Sea Level Test Results Three injectors of the same general design were tested at sea level. Two of the units contained the adjustable film cooling orifices, the third did not provide this capability and operated without film cooling. One of the two units having provision for variable film cooling flow was fabricated with oversize injection orifices and therefore operated at a lower inlet pressure compared to the other two.

The effects of mixture ratio, fuel inlet temperature, chamber length, percent fuel film cooling, and injector pressure drop on the thrust-based specific impulse are shown in Fig. 6. The high ΔP injector operating without film cooling provided a sea level specific impulse (ϵ = 1.6:1) of 2288 ± 5 N-s/kg (233.5 ± 0.5 lb_f-sec/lb_m) at P_c = 690 kN/m^2 (100 psia). Data obtained between O/F = 1.6 and 1.8 and fuel inlet temperatures ranging from 11 to 52°C (52 to 125°F) fell within the ± 5N-s/kg (0.5 lb_f-sec/lb_m) band. Chamber lengths from 9.9 to 11.2 cm (3.9 to 4.4 in.) had no significant effect on performance indicating the vaporization process was essentially complete. This specific impulse translates to a combustion efficiency of 99% at O/F = 1.65 and 99.5% at O/F = 1.50.

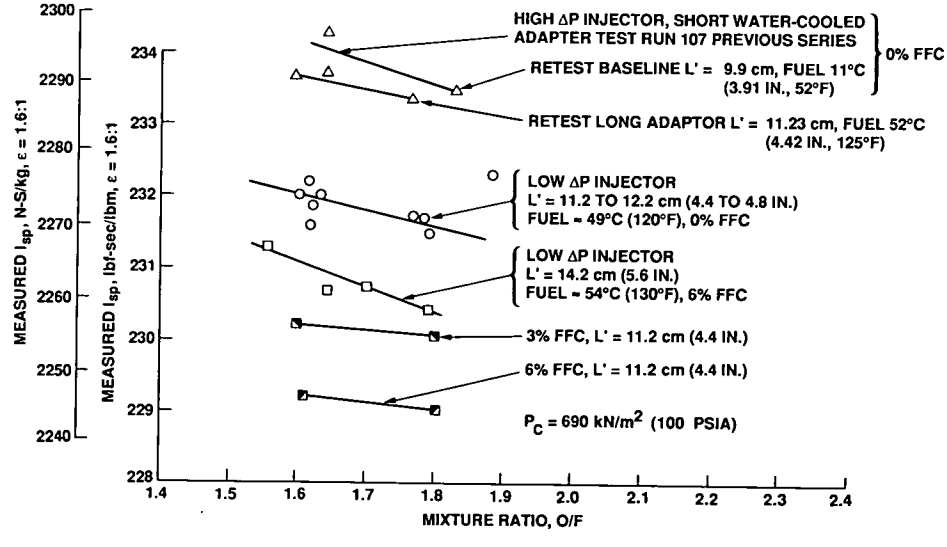

Figure 6. Sea Level I_{sp} vs. Mixture Ratio with Fuel Temperature, Injector ΔP, Chamber Length, and Percent Film Cooling as Independent Parameters (P_c = 690 kN/m^2 (100 psia))

The lower pressure drop injector operating without film cooling demonstrated a specific impulse of 2274 ± 5 N-s/kg (232.0 ± 0.5 lb_f-sec/lb_m) over the same operating envelope. This translates to an efficiency slightly higher than 98%. When the chamber length was increased by 2.54 cm to 14.2 cm (1 in. to 5.6 in.), a performance reduction of 9.8 N-s/kg (1.0 lb_f-sec/lb_m) was measured. The longer cold chamber walls removed more energy than was contributed by the 25% increase in propellant residence time, thus, also, indicating that vaporization was essentially complete for the low pressure drop design.

The addition of 10% fuel film cooling resulted in a specific impulse of 2244 N-s/kg (229 lb_f-sec/lb_m) which translates to an additional 1.5% reduction in efficiency. Tests were also conducted with 6%, 3% and 1.5% fuel film cooling. The maximum amount of fuel film cooling which could be used without measurable performance loss was 1.5%.

The exhaust plume diagnostics indicated the greatest chamber wall chemical compatibility and design margin was obtained at the highest fuel film cooling flows. Under these conditions, no rhenium oxidation was noted at the nominal 1.65 O/F and only minor oxidation was encountered at 1.80 O/F.

The fuel regeneratively cooled head end was connected in series with the valve in most of these tests and performed as predicted and without problem. The preheated fuel supplied to the injector was beneficial to the wall compatibility and had no measurable effect on performance.

Altitude Test Results with ϵ = 44:1 High-Temperature Chamber Performance and thermal mapping tests were conducted with the high pressure drop injector and no film cooling and with the low pressure drop injector with 10.5 and 6.0% fuel film cooling. The high pressure drop injector design delivered a vacuum specific impulse of 3033 ± 1.5 N-s/kg (309.5 ± 0.15 lb_f sec/lb_m) at ϵ = 44:1 after 8 s of chamber heat-up in 3 repeat tests, as shown in Fig. 7. Because the skirt was still cold, further performance increases could be expected with firing time. However, because this initial design did not include the fuel regeneratively cooled head end, the maximum test duration was limited to about 60 s. The maximum observed chamber temperature was under 1816°C (3300°F), well below the 2204°C (4000°F) design limit.

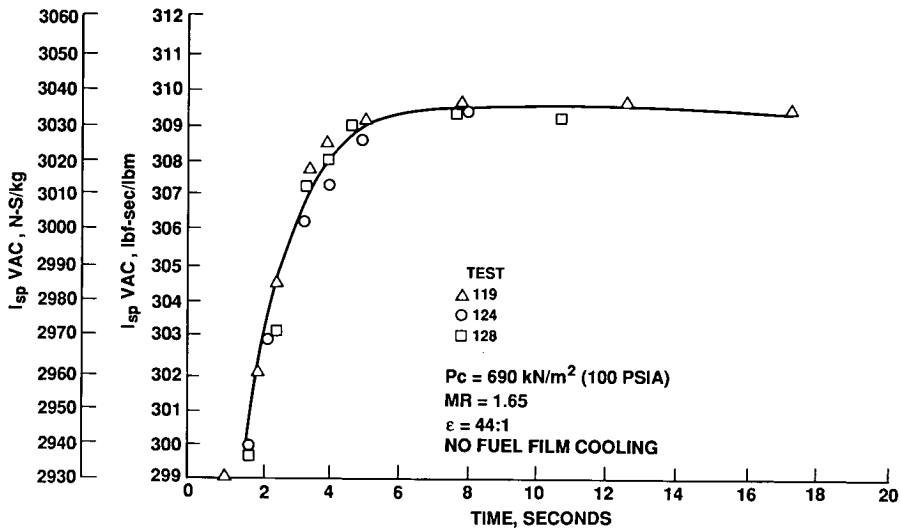

Figure 7. Measured I_{sp} vs. Time, ϵ = 44:1, No Fuel Film Cooling

A series of off-design tests of up to 60 s duration were also conducted. The combustion chamber pressure was varied from 531 to 863 kN/m² (77 to 125 psia) and the O/F from 1.49 to 1.80. The maximum observed temperature did not exceed 1927°C (3500°F) in this operating envelope. Inspection of the high temperature chamber after only 202 s of operation revealed one quadrant at the forward end, which was in a cooler-than-average location, had been severely eroded. Data analysis indicated the erosion was caused by impingement of uncombusted oxidizer on the chamber wall. The remainder of the chamber and the throat were in excellent condition. The chamber was repaired and reused in subsequent testing with a modified head-end design which included the fuel regeneratively cooled transition segment.

The low pressure drop injector was tested with 10% and 6% fuel film cooling with the repaired chamber and the 44:1 nozzle extension. The higher coolant flow yielded an average specific impulse of 2987 N-

s/kg (304.8 lb_f-sec/lb_m) and a maximum temperature of 1649°C (3000°F) in tests which lasted from 50 to 90 S each. With the 6% coolant flow, the I_{sp} increased to 2989 N-s/kg (305.0 lb_f-sec/lb_m), and no measurable increase in maximum operating temperature was recorded. The repaired chamber completed 16 full thermal cycles and accumulated 641 additional seconds of firing at average temperatures between 1538 and 1704°C (2800 and 3100°F) without evidence of degradation.

Durability Testing All experimental data to this point indicated that the design could operate without film cooling, without exceeding the allowable chamber temperature limit of 2204°C (4000°F), and without overheating the head-end attachment. However, because of the uncertainties in the chamber quality due to the manufacturing difficulties and the lack of sufficient test data to verify that the design changes had completely resolved the cause of the earlier head-end oxidation, it was decided to take a more cautious approach to the durability testing. The durability tests were conducted with 5% film cooling and only 14 of the film cooling 16 injectors flowing. Two of the orifices located in a quadrant that had not indicated a head-end oxidation problem without film cooling were deliberately blanked off. Fourteen tests of up to 511 s in duration were conducted on the repaired chamber. Most of the tests were in the 1.5 to 1.54 O/F range. The pressure was varied between 676 and 766 kN/m^2 (98 and 111 psia) to obtain temperature and performance sensitivity data. Maximum temperatures ranged from 1649 to 1927°C (3000 to 3500°F).

The 14 durability tests increased the burn time from 641 to 3381 s. No measurable change in throat diameter was recorded during these tests. However, a large number of small blisters in the ID iridium coating were noted. These blisters formed early in the series of tests and continued to grow in size and number throughout the durability test series. Testing was terminated for more detailed hardware inspection when a number of the blisters were noted to have opened. Since the problem could have been a result of the chamber repair process, a decision was made to continue testing using the second high-temperature chamber. The same injector and valve assembly and film coolant distribution were employed.

The second chamber was fired 33 times to provide a total burn duration of 15,000 s at temperatures ranging from 1856 to 1982°C (3300 to 3600°F). All of the burn time was accumulated at an O/F of 1.65 $\pm$ 0.05. A chamber pressure of 759 $\pm$ 13.8 kN/m^2 (110 $\pm$ 2 psia) was maintained for the first three hours of burn time. In the last 8 tests, of nominal 600 s duration each, the chamber pressure was varied from 683 to 800 kN/m^2 (99 to 116 psia). All test durations were limited by the pumping capability of the vacuum cell and no limiting hardware conditions were encountered. The longest single burn was 823 s. Figure 8 shows some of the measured parameters for the last 675 s test of the durability series. The test program was terminated due to funding limitations.

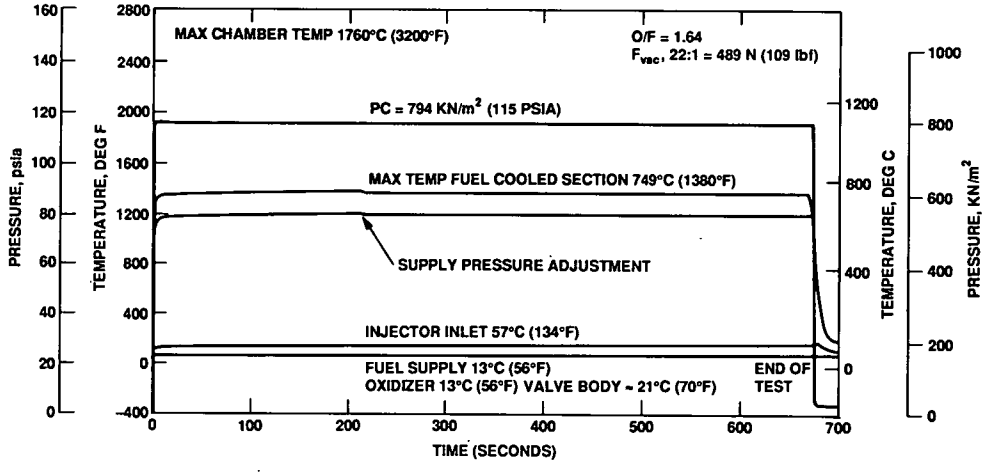

Figure 8. Data from Final 675 s Test of 15,000 s Durability Demonstration

Blister formation similar to the first unit started early in the testing. These enlarged and opened after several hours. Subsequent hours of testing smoothed out the roughened blister zones without any apparent further damage. No blisters were formed at the geometric throat, which maintained dimensional stability within 0.0005 cm (0.0002 in.) throughout the 4 hours. Figure 9 shows the throat viewed from the forward and aft ends of the chamber at the end of the test program.

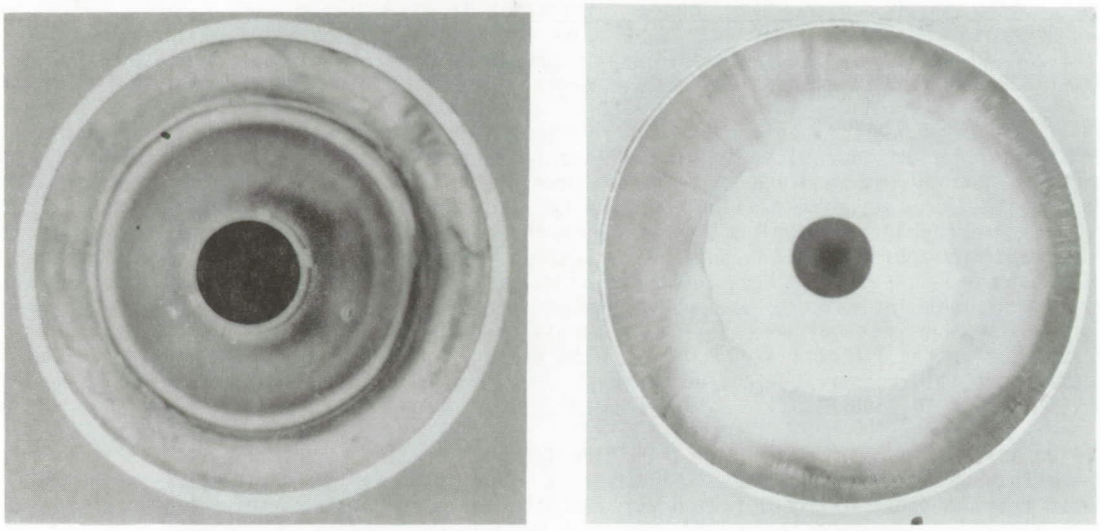

Throat Viewed from Injector End

Throat Viewed from Exit End

Figure 9. High-Temperature Chamber After 15,000 s of Burn Time and 33 Full Thermal Cycles

Extrapolated Performance Extrapolation of the ϵ = 44:1 experimental data to the full ϵ = 467:1 expansion nozzle, using the JANNAF methodology, provides the following performance projections.

The current configuration, operating at 100 psia with the low ΔP injector (S/N 2, 98% efficient) and 6% fuel film cooling, will provide an I_{sp} of 3114 N-s/kg (317.8 lb_f-sec/lb_m) at an ϵ = 467:1. Based on the known thermal design margin, the fuel film cooling can be eliminated. If the high ΔP injector (S/N 1, 99% efficient) is used without film cooling, the specific impulse increases to 3171 N-s/kg (323.4 lb_f-sec/lb_m) at the same operating pressure and with the same nozzle expansion ratio.

Table III defines three projected levels of attainable specific impulse for ϵ = 158:1 and 467:1 configurations. The near-term engine uses the existing injector design, the second generation includes minor improvements to both the injector and chamber designs, while the long-term goals represent the performance attainable after multiple design/optimization iterations and institution of precision fabrication and quality control standards. The projected weight of the engine assembly with the 467:1 nozzle is 4.5 kg (10 lb), including 0.9 kg (2 lb), for the valve.

TABLE III. ATTAINABLE SPECIFIC IMPULSE VS. ENGINE LENGTH AND OPTIMATION EFFORT

Engine Length, cm (in.)	63.5 (25)	99.1 (39)
Expansion Ratio:		
ϵ (Potential Flow)	150:1	400:1
ϵ (Geometric)	158:1	467:1
Exit Diameter, cm (in.)	26.9 (10.6)	46.2 (18.2)
Near-Term, N-s/kg (lb_f-s/lb_m)	3087 (315)	3136 (320)
2nd Generation, N-s/kg (lb_f-s/lb_m)	3116 (318)	3165 (323)
Long-Term Goal, N-s/kg (lb_f-s/lb_m)	3146 (321)	3195 (326)

Durability Based on comparison of the 445 Newton (100 lb_f) and 22 Newton (5 lb_f) experimental results, a durability in excess of 15 hours and 100 starts appears to be easily attainable once the fabrication process quality control for the larger chamber is established. This conclusion is based on the excellent condition of the subscale chamber after 15 hours of burn time at temperatures 260°C (500°F) higher than measured in this 4 hour durability testing effort. Furthermore, the subscale design also sustained thousands of seconds of operation at O/F ratios in the 1.8 to 2.0 range, indicating design margin for operation at higher O/F's without film cooling.

CONCLUSIONS AND RECOMMENDATIONS

A near-perfect injector (η = 99.8%) is required to attain the 3195 N-s/kg (326 lb_f-sec/lb_m) performance at 690 kN/m^2 (100 psia) and 2204°C/1816°C (4000°F/2400°F) chamber/skirt temperatures. Injectors of this efficiency have been demonstrated, but not without difficulty in development and very close control of manufacturing tolerances. The specific impulse with a perfect injector at an O/F = 1.65 is 3202 N-s/kg (326.7 lb_f-sec/lb_m). Several design improvements to increase the performance of the existing injector are possible and specific recommendations have been made.

As an alternate approach, the chamber pressure can be increased from 690 to 1035 kN/m^2 (100 to 150 psia). This will add 22.5 N-s/kg (2.3 lb_f-sec/lb_m) to the attainable performance by reduction of the kinetics-related losses. At the higher pressure, the required injector efficiency is reduced to 99% and this has already been demonstrated. This design approach, however, would not meet the 1587 kN/m^2 (230 psia) inlet pressure goal. An additional 207 to 345 kN/m^2 (30 to 50 psia) will be required. Thus, the remaining activities in this approach would be to establish the minimum injector pressure drop compatible with 99% efficiency and proceed with the fabrication and hot-fire test demonstration of an all-welded 467:1 area ratio to confirm the thermal design and extrapolated specific impulse predictions.

REFERENCES

1. Draper, R., "Comet Rendezvous Asteroid Flyby, First Mariner Mark II," American Astronautical Society, AAS-86-333, October 1986.
2. JPL Publication 400-259, Rev. 1, "A Look Into the Beginning of the Solar System," March 1986.
3. Appel, M. A., Kaplan, R. E., and Tuffias, R. B., "Liquid Fluorine/Hydrazine Rhenium Thruster Update," JANNAF Propulsion Meeting, Monterey, CA, 1983.
4. Appel, M. A., Schoenman, L., and Berkman, D. K., "Oxygen/Hydrogen Thruster for the Space Station Auxiliary Propulsion Systems," JANNAF Propulsion Meeting, New Orleans, LA, 1984.
5. Dowdy, M. W., and Appel, M. A., "High-Temperature Gaseous Oxygen/Hydrogen Thrusters for Space Station."
6. High-Temperature Oxidation-Resistant Materials, NAS 3-24643, to be published.